Design-Stage Analytical And Cfd Assessment Of A Coconut Oil–Fly Ash Composite Pcm Partition Wall With Fan-Assisted Ventilation For Tropical Residential Cooling

Aldissain Jurizat[1*], Usep Surahman[2], Galuh Kresnadian Tedjawinata[3]

[1,2]Architecture, Universitas Pendidikan Indonesia, Jl. Dr. Setiabudhi No. 229, Bandung 40154, Indonesia
[3]Architecture, Universitas Katolik Parahyangan, Jl. Ciumbuleuit No. 94, Bandung 40141, Indonesia
[*] Corresponding author:
Email: aldissain@upi.edu

Abstract.
Masonry dwellings in tropical Indonesia often exceed the indoor comfort range on hot afternoons, encouraging reliance on split-unit air conditioning (AC). This study presents a design-stage assessment of a partition wall containing 918 polyethylene spheres (12 cm) filled with a coconut oil–fly ash composite phase change material (PCM; 50 vol% oil, 40 vol% fly ash, 10 vol% air) and assisted by exhaust fans (24 W in total), for two bedrooms of a Type-36 house in Bandung. A Maxwell-Eucken estimate indicates that fly ash raises the composite thermal conductivity from 0.17 to about 0.32 W/m·K (0.24–0.36 W/m·K). A quasi-steady melting analysis shows that capsule charging is limited mainly by surface convection: the latent heat absorbed during a 5-h afternoon (2.0–3.7 kWh for the whole wall) is similar to that of pure-oil capsules, while the composite uses 44% less oil and completes its melting cycle faster. The installed 373.8 kg of oil corresponds to a theoretical air-temperature reduction of up to 4.0 °C in the 49.5 m³ rooms. A steady-state CFD simulation (Butterfly/OpenFOAM) for the EPW design hour (9 December, 14:00; outdoor 29.0 °C), with the PCM surface prescribed at 25.5 °C, gives an indoor air temperature of 26.33 °C against 28.30 °C for brick partitions, within the ASHRAE 55 adaptive comfort limits. Operating electricity and CO_2 emissions are 95–97% lower than for two ½ PK AC units, with a simple payback of about 3.3 years; as the AC provides lower temperatures and dehumidification, these are upper bounds. Transient coupled simulation and prototype testing are required for validation.

Keywords: *Phase change material, coconut oil, fly ash, partition wall, CFD and tropical housing.*

I. INTRODUCTION

Space cooling is the fastest-growing end use of energy in buildings; air conditioners and electric fans already account for nearly one-fifth of the electricity used in buildings worldwide, and Indonesia is among the countries where the stock of air conditioners is projected to grow most rapidly [1]. In Indonesia, brick masonry is the prevailing construction method for low- and middle-income housing. Heavy masonry walls store solar and internal heat gains during the day and release them into the interior through the afternoon and evening [2, 3], so that indoor air temperatures in such dwellings often remain above the comfort range and occupants turn to split-unit air conditioning.

Phase change materials (PCMs) absorb and release latent heat at a nearly constant temperature during the solid–liquid transition [4, 5]. When the transition temperature lies within the comfort range, PCM-integrated components can attenuate indoor temperature peaks and reduce cooling loads; reviews report load reductions of up to about 30% [2, 4], and simulations for tropical Singapore have quantified the cooling-load benefit of PCM-integrated envelopes [6]. Coconut oil has been identified as a suitable bio-based organic PCM for tropical and subtropical climates because its melting range lies close to indoor comfort temperatures [7, 8], and experimental work in Indonesia has demonstrated its potential for indoor air-temperature control [9–11]. Coconut oil has also been combined with porous bio-based supports to form composite PCMs for building envelopes [12], and encapsulation is the usual route to integrating PCMs into construction materials [13].

Two physical constraints limit the use of coconut oil PCM in Indonesian dwellings. The first is a material-rate constraint. Like most organic PCMs, coconut oil has a low thermal conductivity (about 0.17–0.19 W/m·K [8]), so the rate at which its latent heat can be charged or discharged is limited by conduction through the bulk material [5]. Inorganic fillers such as fly ash have been used as supports in shape-stabilised PCMs and can increase composite conductivity; for a polyethylene glycol/fly ash composite, an increase of 48.6% has been reported [14], and fly ash has also been combined with PCMs in foam concrete [15]. The second is an airflow constraint: under still indoor air, heat exchange between the PCM surface and the room air relies on natural convection with low heat-transfer coefficients (typically 2–5 W/m²·K), whereas even

modest forced airflow increases the coefficient several-fold. Dynamic and fan-assisted PCM envelopes have been proposed for this reason [16, 17]. The use of fly ash as a filler also redirects a coal-combustion residue, which is no longer classified as hazardous waste in Indonesia when produced by non-stoker boilers [18], into a building product.

This study addresses both constraints for a partition wall containing polyethylene-encapsulated coconut oil–fly ash composite and assisted by low-power exhaust fans. Four research questions are posed: (1) By how much does fly ash theoretically increase the composite thermal conductivity, and does this translate into faster charging of a 12 cm capsule under realistic surface heat-transfer conditions? (2) For a Type-36 dwelling in Bandung, what mass of coconut oil is required for a 2 °C air-temperature reduction, and does the encapsulated mass meet it? (3) With the PCM surface at its melting temperature and the fans operating, what indoor air temperature and air-velocity field does a CFD simulation predict at the design hot hour? (4) How do the operating energy, CO_2 emissions and costs compare with split-unit air conditioning?

The study is deliberately framed as a design-stage assessment. Analytical calculations address the material and capacity questions; a steady-state CFD simulation addresses the airflow question with the PCM surface represented by a prescribed temperature. The latent-heat dynamics are therefore not resolved in the CFD, and the results are not a validation of the system. Prior work by the first author measured an indoor temperature reduction rate of 0.87 °C/h for coconut oil used as internal thermal mass in a brick house [3]; the present study extends this to a composite PCM in spherical capsules.

II. METHODS

2.1 PCM composite composition

Each spherical capsule contains three components by volume: 50% coconut oil, 40% fly ash and 10% residual air. Coconut oil is the latent-heat storage medium; refined coconut oil melts at 24.5 ± 1.5 °C with a bulk melting range of about 21–27 °C and a latent heat of 105 ± 11 kJ/kg [8], while Wonorahardjo et al. reported a melting point of about 26 °C [9]. Fly ash is added to raise the thermal conductivity of the composite (Section 2.3). Indonesian coal fly ashes are dominated by SiO_2 and Al_2O_3: XRF analyses report SiO_2 43.8%, Al_2O_3 23.0%, Fe_2O_3 10.6%, CaO 10.2% and MgO 4.3% for Suralaya fly ash (ASTM C618 Class F) [19], and SiO_2 43.7%, Al_2O_3 21.0%, Fe_2O_3 22.5%, CaO 4.9% and MgO 2.6% for Asam-Asam fly ash [20]. These are glassy and crystalline mineral oxides rather than metallic conductors; their benefit lies in a solid-phase conductivity higher than that of the oil. Because composition varies between power plants, the fly ash used should be characterised by XRF in the experimental stage. The 50:40 ratio was selected from earlier mixing trials, balancing thermal enhancement against cost [21].

Polyethylene (PE) spheres with a 12 cm diameter serve as the encapsulation, based on an earlier study of capsule sizes for encapsulated coconut oil [22]. PE is chemically compatible with both components and is commercially available at low cost (about IDR 2,500 per unit).

2.2 Capsule volume and material quantities

The volume of each sphere (r = 6 cm) is:

$$V = (4/3)\cdot\pi\cdot r^3 = (4/3) \times 3.1416 \times 6^3 = 904.78\ \text{cm}^3 \quad (1)$$

Because manual filling does not use the full volume, a fill efficiency of 90% gives an effective fill volume V_t = 814.30 cm³ per capsule. Expressed as fractions of the sphere volume, the components per capsule are:

$$V_{oil} = 0.50\ V = 452.39\ \text{cm}^3 \quad (2a)$$

$$V_{fa} = 0.40\ V = 361.91\ \text{cm}^3 \quad (2b)$$

$$V_{air} = 0.10\ V = 90.48\ \text{cm}^3 \quad (2c)$$

so that $V_{oil} + V_{fa} = V_t$. For the 918 capsules the totals are 415.3 L of coconut oil and 332.2 L of fly ash. With the density of coconut oil $\rho_{oil} \approx 0.90$ kg/L [8], the installed oil mass is:

$$M_{oil} = 415.3\ \text{L} \times 0.90\ \text{kg/L} \approx 373.8\ \text{kg} \quad (3)$$

For comparison, the same 918 capsules filled with pure oil at 90% fill would contain about 672.8 kg of oil.

2.3 Composite thermal conductivity and response time

The effective conductivity of the composite was estimated with the Maxwell-Eucken model in the form given by Wang et al. [23]:

$$k_{eff} = k_m [2k_m + k_p + 2\varphi(k_p - k_m)] / [2k_m + k_p - \varphi(k_p - k_m)] \quad (4)$$

where k_m is the matrix conductivity, k_p the dispersed-phase conductivity and φ its volume fraction. The model was applied sequentially: first fly ash in oil ($\varphi = 0.40/0.90 = 0.444$), then the 10 vol% air (k_{air} = 0.026 W/m·K) in the oil–fly ash mixture. The oil conductivity was taken as 0.17 W/m·K (liquid) [8]. No verified value was found for the conductivity of solid fly ash particles; published values for fly ash powders refer to the porous bulk material and are much lower. A central value of k_p = 1.0 W/m·K, typical of aluminosilicate glass, was therefore assumed, with a sensitivity range of 0.5–1.5 W/m·K.

The thermal diffusivity $\alpha = k/(\rho c)$ was computed with ρc_{oil} = 900 kg/m³ × 1.9 kJ/kg·K (mean of the solid and liquid specific heats, 1.6 and 2.2 kJ/kg·K [8]) and, for fly ash, ρ = 2,200 kg/m³ and c = 0.72 kJ/kg·K [24], giving $\rho c_{composite}$ = 1.49 MJ/m³·K. The conduction time scale $\tau = R^2/\alpha$ of a capsule of radius R = 6 cm is a sensible-heat indicator only, because it ignores latent heat.

To account for latent heat, the time required to melt the capsule was estimated with the quasi-steady (low Stefan number) approximation for inward melting of a sphere [25], including the convective resistance at the capsule surface. For a melt front at radius r, the elapsed time is:

$$t(r) = (\rho L)_v/\Delta T \times [\, (R^3 - r^3)/(3hR^2) + (1/k)((R^2 - r^2)/2 - (R^3 - r^3)/(3R)) \,] \quad (5)$$

where $(\rho L)_v$ is the volumetric latent heat of the capsule contents (0.50 × 900 × 105 kJ/m³ for the composite and 0.90 × 900 × 105 kJ/m³ for pure oil), ΔT is the difference between the cavity air temperature and the melting temperature, h is the surface heat-transfer coefficient and k the conductivity of the molten region. The thin PE shell, natural convection inside the molten oil, and settling of fly ash are neglected. Cases with h = 5–10 W/m²·K (natural to weak forced convection) and ΔT = 2–3 K were evaluated, and the fraction of the capsule melted within a 5-h afternoon was obtained by inverting Eq. (5).

2.4 Latent-heat capacity

Wonorahardjo et al. [9] derived an experimental thermal mass capability of coconut oil for air temperature control of x = 0.533 K·m³/kg, defined by $\Delta T_a = (x/V_r)\cdot m$. The mass required for a target reduction ΔT in a room of volume V_r is therefore:

$$M_{required} = \Delta T \times V_r / x \quad (6)$$

For the combined room volume V_r = 49.5 m³ (Section 2.5) and ΔT = 2 °C, $M_{required}$ = 99/0.533 ≈ 185.7 kg. The installed 373.8 kg exceeds this by 188.0 kg (+101%), and the corresponding theoretical maximum reduction is:

$$\Delta T_{max} = x \times M_{oil} / V_r = 0.533 \times 373.8 / 49.5 \approx 4.02\ °C \quad (7)$$

The empirical coefficient x was obtained for a specific experimental room and implicitly includes its envelope heat gains; Eq. (7) is therefore an indicator of reservoir size rather than a prediction. The total latent heat stored in the installed oil is 373.8 kg × 105 kJ/kg ≈ 39.2 MJ (10.9 kWh). Table 2 summarises the capacity calculation.

2.5 Building model and wall system

The PCM partition walls (Fig. 1) replace the conventional walls separating two adjacent bedrooms of a standard Indonesian Type-36 dwelling (Fig. 2). The two bedrooms have a combined floor area of 16.5 m² and a ceiling height of 3.0 m, i.e. a combined volume V_r = 49.5 m³.

The PCM wall uses a double galvanised hollow-steel frame (40 × 40 × 2 mm sections) in 60 × 120 cm modules. Each module holds 27 capsules supported on wooden shelving and is clad on both sides with 9 mm gypsum board. The system comprises three wall sections — Wall A (405 capsules, 15 modules), Wall B (297 capsules, 11 modules) and Wall C (216 capsules, 8 modules) — for a total of 918 capsules in 34 modules (about 24.5 m² of wall). Two exhaust fans, one serving each bedroom, are mounted at the top of the wall and draw room air through the capsule cavity; their combined rated input, including power supplies, is 24 W (12 W each).

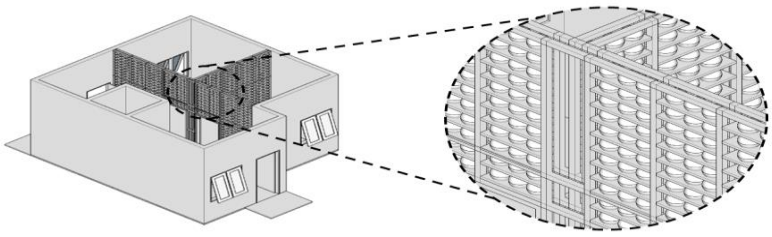


Fig. 1. PCM partition wall installed between two adjacent bedrooms of the Type-36 model, with detail of the capsule arrangement

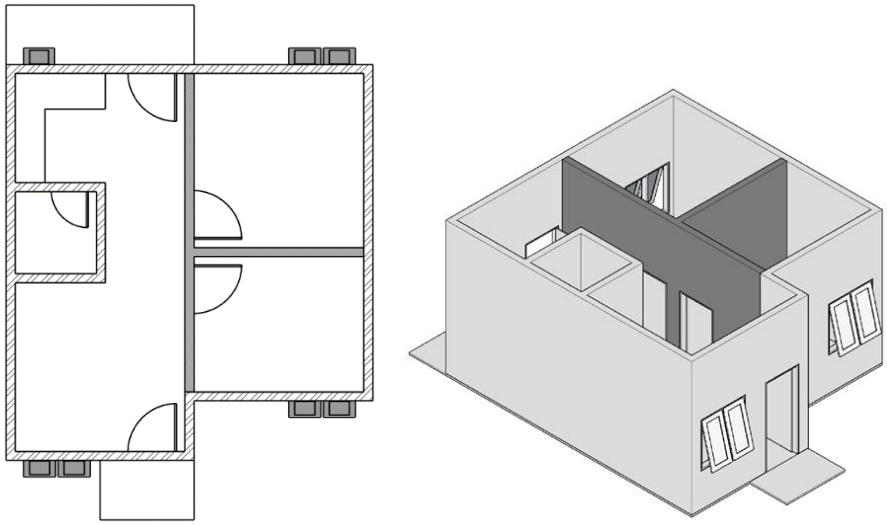


Fig. 2. (a) Floor plan of the Type-36 dwelling; (b) baseline model with conventional brick partition walls

2.6 Climate data and design hour

Boundary conditions were taken from the EnergyPlus weather (EPW) file for Bandung (station 967830, ISD-TMYx; latitude −6.883°, longitude 107.600°, elevation 791 m). The file header identifies 26 March–1 April as the typical week and 3–9 December as the extreme hot week. A few physically implausible records elsewhere in the file ($T > 35$ °C with RH ≥ 90% on 12 June, 24 June and 7 July) were noted and excluded. Within the extreme hot week, 9 December at 14:00 local standard time was selected as the design hour (Table 3), because the daily profile is smooth (23.1 °C minimum overnight, 29.0 °C peak at 14:00) and because the concurrent conditions — RH 61% and global horizontal radiation 612 Wh/m² — describe a clear, hot afternoon.

Table 3. Design-hour boundary conditions (Bandung EPW 967830, 9 December, 14:00 LST)

Parameter	Value	Unit
Outdoor dry-bulb temperature	29.0	°C
Relative humidity	61	%
Global horizontal radiation	612	Wh/m²
Daily mean temperature (9 December)	25.6	°C
Hour of year	8222	–

2.7 CFD simulation

Airflow and air temperature were simulated with Rhinoceros 7, Grasshopper and the Butterfly plug-in, which interfaces with the OpenFOAM finite-volume solver. The steady-state incompressible Navier–Stokes equations were solved with energy transport and buoyancy using Butterfly's heat-transfer recipe, which runs the OpenFOAM solver buoyantBoussinesqSimpleFoam (steady state, Boussinesq approximation for buoyancy) with the RNG k–ε RANS turbulence model and a residual target of 10^{-4} for all quantities [26]. The mesh was generated with blockMesh and snappyHexMesh through Butterfly; a formal mesh-independence study was not performed (Section 3.6). The outdoor dry-bulb temperature of the design hour (29.0 °C) from the EPW file was applied as the external boundary temperature, and a wind speed of 0.384 m/s was applied at the openings in both scenarios; solar radiation was not modelled explicitly.

Two scenarios were simulated under identical EPW conditions: Scenario 1, the baseline with half-brick partition walls, in which the partition surface temperature results from the conduction–convection balance of the wall; and Scenario 2, the PCM wall with fans. In Scenario 2 the air discharged by the fans from the capsule cavity into each room is represented as an inlet boundary with a fixed temperature of 25.5 °C, within the melting range of coconut oil, and a velocity corresponding to the rated fan flow. This treats the cavity as an air-to-PCM heat exchanger whose outlet air leaves at the melting temperature while the PCM is melting; the assumption is examined in Section 3.2. The capsule assembly is represented as a continuum zone with an effective density $\rho_{eff} = 0.50\rho_{oil} + 0.40\rho_{fa} + 0.10\rho_{air}$. Air temperature and velocity were evaluated as area averages over a horizontal plane at 1.0 m above the floor. Simulations were repeated until the velocity field no longer changed between successive runs, and Run 8 was taken as the converged solution.

The analytical and CFD stages are complementary rather than cross-validating. They are linked by a single assumption — that the PCM surface remains near the melting temperature during the design hour — which Sections 2.3 and 2.4 support only approximately. A scenario with the same cavity and fans but without PCM, which would isolate the PCM contribution, could not be performed in this study and is a stated limitation (Section 3.6).

III. RESULTS AND DISCUSSION

3.1 Composite conductivity and capsule charging

Table 1 shows that the Maxwell-Eucken model predicts a composite conductivity of 0.32 W/m·K for the central particle conductivity (1.9 times that of pure oil), with a range of 0.24–0.36 W/m·K (1.4–2.1 times) over the assumed particle values. Because fly ash also has a lower volumetric heat capacity than the oil it replaces, the diffusivity increases by 1.6–2.4 times, and the conduction time scale τ falls from about 10 h to 4–6 h.

Table 1. Estimated thermal properties of pure coconut oil and of the composite (50 vol% oil, 40 vol% fly ash, 10 vol% air)

Property	**Pure oil**	**Composite, k_p = 0.5**	**Composite, k_p = 1.0**	**Composite, k_p = 1.5**
Thermal conductivity k (W/m·K)	0.17	0.24	0.32	0.36
Ratio to pure oil	1.00	1.43	1.86	2.10
Thermal diffusivity α (10^{-7} m²/s)	0.99	1.63	2.13	2.40
Conduction time scale τ = R^2/α (h)	10.1	6.1	4.7	4.2

Note: k_p: assumed conductivity of solid fly ash particles (W/m·K).

Fig. 3 places the design mix within the trade-off it creates: conductivity rises with fly ash content (Fig. 3a), but the latent heat stored per unit capsule volume falls in direct proportion to the oil displaced (Fig. 3b).

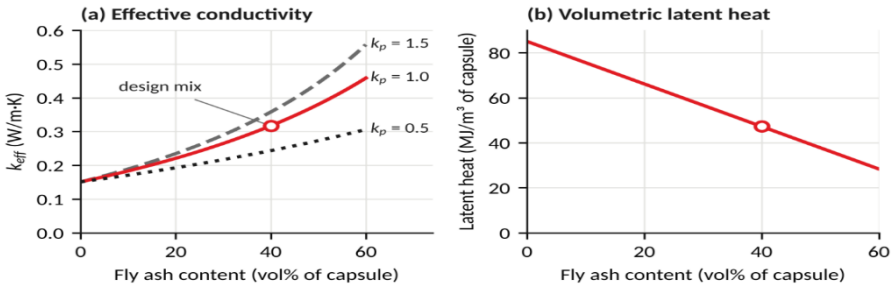


Fig. 3. Effect of fly ash content on (a) the effective conductivity of the capsule contents for three assumed particle conductivities k_p (W/m·K) and (b) the volumetric latent heat; the circle marks the design mix (40 vol%)

The latent-heat analysis (Table 2b) changes the interpretation of this enhancement. With surface coefficients of 5–10 W/m²·K, the convective resistance at the capsule surface is comparable to or larger than the conduction resistance of the molten layer (Biot number hR/k ≈ 1–2), so charging is limited mainly by surface convection. Full melting of a composite capsule requires 17–39 h, against 44–89 h for a pure-oil capsule; within a 5-h afternoon, 18–48% of a composite capsule melts, against 10–27% of a pure-oil capsule. Because the composite stores less latent heat per capsule, the energy absorbed by the whole wall in 5 h is nearly the same in both cases: about 2.0 kWh at h = 5 W/m²·K and 3.7 kWh at h = 10 W/m²·K (ΔT = 2 K), i.e. an average absorption of roughly 400–740 W (Fig. 4). The practical benefits of fly ash are therefore that it achieves this afternoon absorption with 44% less oil (373.8 kg instead of 672.8 kg), which reduces cost and fire load, and that the shorter full cycle makes complete overnight re-solidification more attainable. The analysis also shows that raising the surface heat-transfer coefficient — the role of the fans — has a larger effect on daily absorption than raising the bulk conductivity.

Table 2. (a) Latent-heat capacity and (b) estimated capsule charging for the installed wall

Parameter	Value	Unit
(a) Total coconut oil volume (918 capsules)	415.3	L
Total coconut oil mass	373.8	kg
Combined room volume	49.5	m³
Thermal mass capability x [9]	0.533	K·m³/kg
Minimum oil mass for ΔT = 2 °C	185.7	kg
Surplus over minimum	+188.0 (+101%)	kg
Theoretical maximum ΔT	4.02	°C
Total stored latent heat	39.2 (10.9)	MJ (kWh)
(b) Full-melt time, composite / pure oil	17–39 / 44–89	h
Fraction melted in 5 h, composite / pure oil	0.18–0.48 / 0.10–0.27	–
Latent heat absorbed in 5 h, whole wall (ΔT = 2 K, h = 5–10 W/m²·K)	2.0–3.7 (both fillings)	kWh

Note: Part (b): quasi-steady estimate, Eq. (5), h = 5–10 W/m²·K and ΔT = 2–3 K unless stated.

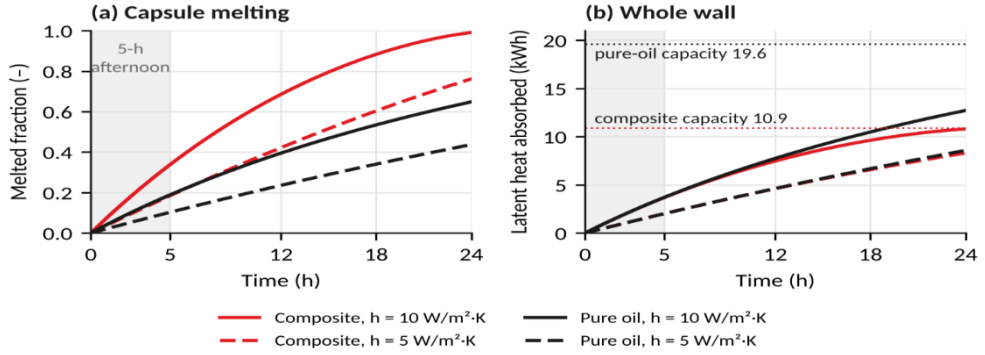


Fig. 4. Quasi-steady charging of composite and pure-oil capsules (ΔT = 2 K): (a) melted fraction of a capsule; (b) latent heat absorbed by the whole wall, with the total latent capacities shown dotted. The shaded band marks a 5-h afternoon

3.2 CFD results: air temperature and velocity

In the baseline (Scenario 1), the simulated indoor air temperature at the design hour is 28.30 °C, 0.70 °C below the outdoor temperature, and the mean air velocity is 0.384 m/s. With the PCM wall and fans (Scenario 2), the indoor air temperature falls to 26.33 °C (ΔT = 1.97 °C) and the mean velocity rises to 0.426 m/s (+0.042 m/s, +10.9%) (Table 4; Figs. 5 and 6).

Table 4. CFD results at 1.0 m height: brick baseline (Scenario 1) and PCM wall with fans (Scenario 2)

Parameter	Scenario 1 (brick)	Scenario 2 (PCM + fans)
Indoor air temperature (°C)	28.30	26.33
Reduction relative to outdoor 29.0 °C (°C)	0.70	2.67
Reduction relative to Scenario 1 (°C)	–	1.97
Mean air velocity (m/s)	0.384	0.426 (+10.9%)

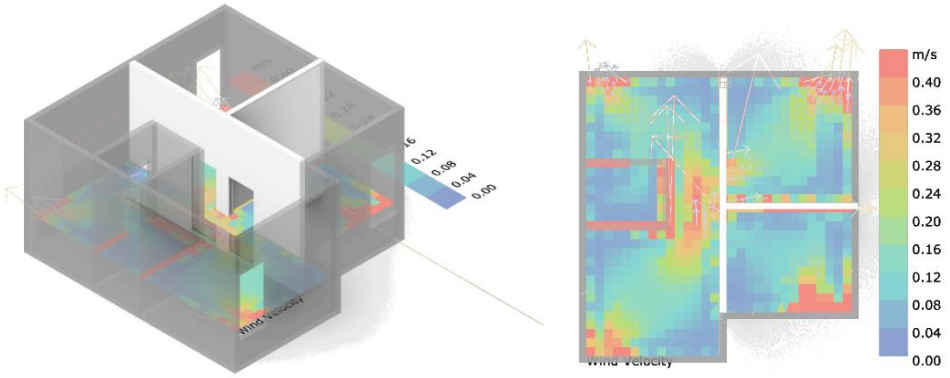


Fig. 5. Air-velocity field for the baseline with brick partition walls (Scenario 1): (a) isometric view; (b) plan at 1.0 m

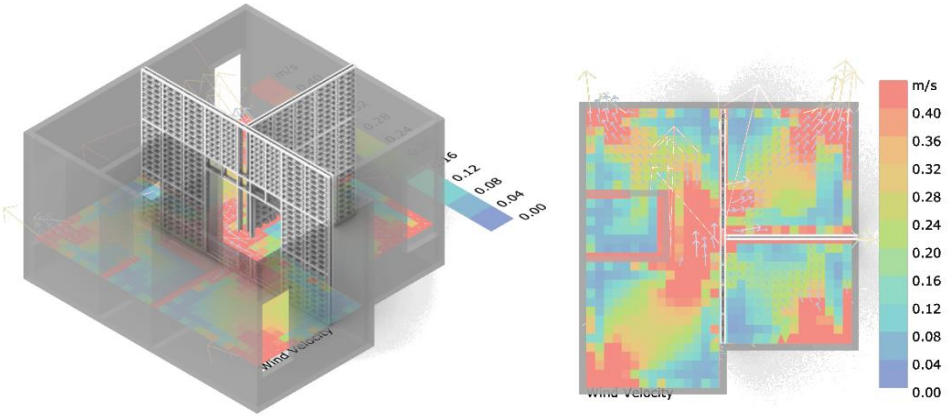


Fig. 6. Air-velocity field for the PCM wall with fans (Scenario 2): (a) isometric view; (b) plan at 1.0 m

The simulated reduction must be read within the limits of the method. Because the PCM surface is held at 25.5 °C, the CFD result describes the sensible cooling that a surface at the melting temperature, combined with the fan-driven airflow, would deliver; it does not show that the PCM can maintain that surface temperature. Two checks support the fixed inlet temperature. First, the cavity behaves as a heat exchanger with a large transfer area: the 918 spheres expose 41.5 m², giving UA ≈ 210–420 W/K for h = 5–10 W/m²·K. For an assumed flow of 70–150 m³/h per fan (typical of 120 mm DC fans), the air capacity rate is 47–101 W/K, the number of transfer units NTU = UA/($\dot{m}c_p$) is 2.1–8.9 and the effectiveness ε = 1 − exp(−NTU) is 0.87–1.00, so the discharged air approaches the PCM temperature. Second, the heat delivered to the PCM by this airflow, $\dot{m}c_p\varepsilon(T_{room} - 25.5\ °C)$, is 40–280 W for room temperatures between 26.3 and 28.3 °C. This is below the 400–740 W that the capsules can absorb (Section 3.1), and over 8 h of operation it amounts to at most about 2.2 kWh, a fifth of the 10.9 kWh latent capacity. The reservoir is therefore not exhausted during the design hour. Comparing the surface heat flux from a transient simulation with these estimates remains the most direct check and is recommended in the next stage. Furthermore, because the cavity, the PCM and the fans were changed together, the 1.97 °C reduction cannot be attributed to the PCM alone; part of it may arise from the lighter gypsum wall and the increased air movement.

Comfort was assessed against two references. In SNI 03-6572-2001, the effective-temperature bands are 22.8–25.8 °C for optimal comfort and 25.8–27.1 °C for warm comfort [27]; the Scenario 2 air temperature (26.33 °C) lies in the warm-comfort band, whereas the baseline (28.30 °C) lies above it, although air temperature is only a proxy for effective temperature. Under the ASHRAE 55 adaptive model,

$T_{comf} = 0.31T_{pma} + 17.8$ °C with acceptability limits of ±2.5 °C (90%) and ±3.5 °C (80%) [28]. Taking the design-day mean (25.6 °C) as the prevailing mean outdoor temperature gives upper limits of 28.2 °C (90%) and 29.2 °C (80%); with a lower prevailing mean of 23 °C they are 27.4 °C and 28.4 °C. Scenario 2 is within all of these limits, while the baseline exceeds the 90% limit. Air temperature rather than operative temperature was evaluated, and no elevated-air-speed allowance was applied; a PMV/PPD or operative-temperature assessment [29] would refine this conclusion. Fig. 7 shows both scenarios against the adaptive comfort bands.

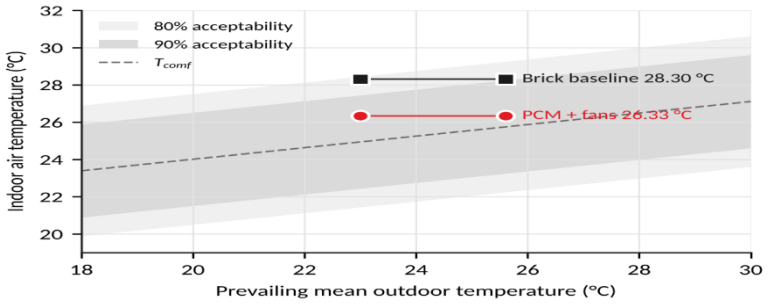


Fig. 7. Simulated indoor air temperatures of the two scenarios against the ASHRAE 55 adaptive comfort bands, for prevailing mean outdoor temperatures of 23.0 and 25.6 °C

3.3 Overnight regeneration

A PCM wall works only if the material re-solidifies between hot days. On the design day the outdoor minimum is 23.1 °C, close to the lower end of the coconut oil melting range. Kahwaji and White reported only 0.9 K of supercooling in a 15 mL bulk sample [8], but Wonorahardjo et al. observed solidification at about 17 °C [9], and full-cycle times of 17–39 h for the composite (Table 2) exceed a single night. Complete regeneration in Bandung therefore cannot be assumed. Operating the fans at night to draw cooler air through the cavity (night flushing) is a low-cost measure that the present configuration already allows; its effectiveness should be evaluated in a transient simulation.

3.4 Operating energy and CO_2 emissions

The baseline cooling system consists of two ½ PK split units with a combined rated input of 640–800 W, operated 8 h per day. The PCM system uses exhaust fans with a total rated input of 24 W, also operated 8 h per day. The daily electricity use is:

$$E_{AC} = P_{AC} \times t \times d = 0.72\ \text{kW} \times 8\ \text{h} \times 1.0 = 5.76\ \text{kWh/day} \quad (8)$$

$$E_{fan} = 0.024\ \text{kW} \times 8\ \text{h} = 0.192\ \text{kWh/day} \quad (9)$$

where d is the compressor duty factor. The central case uses the mid-range rated input (720 W) and d = 1.0; the range covers 640 W with d = 0.7 (3.58 kWh/day) to 800 W with d = 1.0 (6.40 kWh/day). The relative reduction in operating electricity is:

$$\text{Reduction} = (1 - E_{fan}/E_{AC}) \times 100\% = (1 - 0.192/5.76) \times 100\% \approx 96.7\% \quad (10)$$

with a range of 94.6–97.0%. CO_2 emissions were calculated with the grid emission factor of the Jawa-Madura-Bali system, 0.87 kg CO_2/kWh for 2019, published by the Ministry of Energy and Mineral Resources [30]. Because both systems draw electricity from the same grid, the relative emission reduction equals the relative energy reduction and does not depend on the factor chosen; the absolute values scale linearly with it, and using the combined-margin value of 0.891 kg CO_2/kWh calculated for the same grid [31] would change them by less than 3%. Annual figures (365 days) are given in Table 5.

Table 5. Operating electricity and CO_2 emissions for the two bedrooms (8 h/day, 365 days/year)

Parameter	AC system	PCM + fans
Equipment	2 × ½ PK split unit	Exhaust fans with power supplies
Rated input (W)	640–800	24
Electricity (kWh/day), central [range]	5.76 [3.58–6.40]	0.192
Electricity (kWh/year), central [range]	2,102 [1,308–2,336]	70.1
CO_2 (kg/year) at 0.87 kg/kWh, central [range]	1,829 [1,138–2,032]	61.0
Reduction in electricity and CO_2	–	96.7% [94.6–97.0%]

These figures compare operating electricity only and should be read as upper bounds on the savings. The AC systems can hold a lower set-point and remove moisture (outdoor RH at the design hour is 61%), whereas the PCM system reaches 26.33 °C at the design hour and does not dehumidify; the two systems do not provide an identical service.

3.5 Cost comparison

Table 6 compares capital and operating costs. The AC scenario retains brick partition walls; the PCM scenario replaces them with the steel-frame gypsum wall, capsules and fans. Electricity was priced at the R-1 household tariff for 1,300 VA and above, IDR 1,444.70/kWh [32]. AC servicing was assumed to be quarterly cleaning at IDR 100,000 per unit per visit; the PCM maintenance allowance (IDR 273,040 per year) covers fan and power-supply replacement. The brick partition was costed at an indicative IDR 430,000/m² for a half-brick wall with plaster, skim coat and paint on both sides, built up from the national AHSP work items [33] at indicative 2024–2025 unit prices, applied to the same 24.5 m² of wall; a ±20% range is considered.

Table 6. Capital and annual operating costs (IDR)

Cost component	AC system	PCM + fans
Partition wall (brick / steel frame and gypsum)	10,526,400	18,363,824
Cooling units / PCM capsules and fans	8,475,270	11,993,138
Capital cost	19,001,670	30,356,962
Electricity (per year)	3,037,337	101,245
Servicing / maintenance (per year)	800,000	273,040
Operating cost (per year)	3,837,337	374,285
Total, year 1	22,839,007	30,731,247
Cumulative, 5 years	38,188,356	32,228,385
Cumulative, 10 years	57,375,043	34,099,808

Note: Brick-wall cost (IDR 430,000/m²) and AC servicing are indicative assumptions (see text).

The PCM system has a higher capital cost (about IDR 11.4 million more) but saves about IDR 3.46 million per year in operating cost, giving a simple payback of about 3.3 years (2.7–3.9 years for brick-wall costs ±20%); it is more expensive in the first three years and cheaper from the fourth year onward (Fig. 8). Replacement of capsules and oil, AC replacement, discounting and electricity-tariff changes are not included.

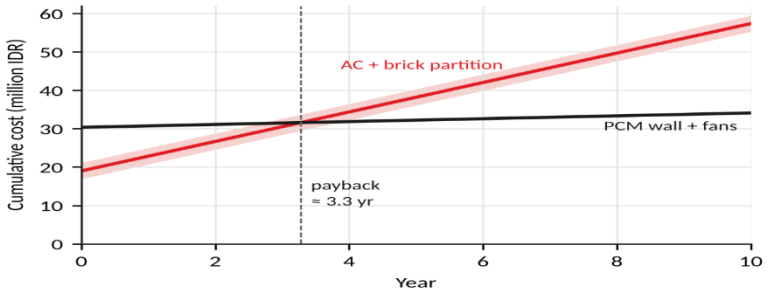


Fig. 8. Cumulative capital and operating cost of the two systems over ten years; the shaded band shows the AC scenario for brick-wall costs ±20%

3.6 Limitations and future work

The following limitations bound the conclusions of this design-stage study and define the next steps.

(a) Prescribed PCM boundary and CFD set-up. The steady-state CFD fixes the temperature of the air leaving the PCM cavity at 25.5 °C. Although Section 3.2 indicates that this is plausible, a transient simulation with an enthalpy–porosity model of the capsules is needed to confirm it. The CFD set-up should also be strengthened by a mesh-independence study, explicit solar gains on the envelope, documented opening conditions and temperature contour plots.

(b) Missing control scenario. A scenario with the same cavity and fans but without PCM (or with an inert filler) was not performed. Without it, the contributions of the wall construction, the PCM and the fans to the 1.97 °C reduction cannot be separated.

(c) Diurnal cycle and regeneration. A 24-h transient simulation is required to establish whether the PCM re-solidifies overnight in Bandung, with and without night flushing.

(d) Material properties. The conductivity of the fly ash particles was assumed, settling of fly ash in the molten oil and long-term oxidation of the oil were not considered, and the composite properties should be measured (transient hot-wire or guarded hot-plate methods, DSC over repeated cycles). Experimental studies of PCM building prototypes [34] provide suitable protocols.

(e) Safety and structure. The installed oil represents a fire load of roughly 14 GJ (373.8 kg × about 38 MJ/kg, a typical higher heating value of vegetable oils [35]), comparable to the ordinary fire load of the two bedrooms, and the oil and fly ash add of the order of one tonne to the lightweight partition. Fire resistance of the cladding, capsule leakage and the structural capacity of the frame must be verified before field installation.

(f) Physical validation. An instrumented prototype in a representative Type-36 dwelling, monitoring indoor and outdoor conditions, PCM surface temperatures, fan power and occupant comfort, is required to validate the results.

IV. CONCLUSION

This design-stage study assessed a coconut oil–fly ash composite PCM partition wall with low-power exhaust fans for two bedrooms of a Type-36 dwelling in Bandung. The Maxwell-Eucken model indicates that 40 vol% fly ash raises the composite conductivity from 0.17 to about 0.32 W/m·K (0.24–0.36 W/m·K over the assumed particle conductivity). Under realistic surface heat-transfer coefficients, however, capsule charging is limited mainly by surface convection: the composite absorbs about the same latent heat during a 5-h afternoon as capsules of pure oil (2.0–3.7 kWh for the whole wall) while using 44% less oil and completing its melting cycle faster. Increasing the surface heat-transfer coefficient, which is the role of the fans, is the more effective lever.

The installed 373.8 kg of coconut oil exceeds the 185.7 kg required for a 2 °C reduction in the 49.5 m³ rooms, with a theoretical maximum reduction of 4.0 °C. With the PCM surface prescribed at 25.5 °C and the fans operating, the steady-state CFD simulation for the design hour gives an indoor air temperature of 26.33 °C compared with 28.30 °C for brick partitions, within the ASHRAE 55 adaptive comfort limits and the SNI 03-6572-2001 warm-comfort band. Compared with two ½ PK AC units operated for the same hours, operating electricity and CO_2 emissions are about 95–97% lower, and the higher capital cost is recovered in about 3.3 years; because the systems do not provide an identical service, these figures are upper bounds.

The results support the concept but do not validate it. A transient coupled simulation, a control scenario without PCM, assessment of overnight regeneration, measurement of the composite properties, fire and structural checks, and an instrumented prototype are the required next steps.

V. ACKNOWLEDGMENTS

The authors gratefully acknowledge Universitas Pendidikan Indonesia for institutional support. An earlier version of this work was presented at the Bukit Asam Innovation Award 2022: Greenovator.

Author contributions. Aldissain Jurizat: conceptualization, methodology, calculation, simulation, writing – original draft. Galuh Kresnadian Tedjawinata: model design, visualization. Usep Surahman: data collection, writing – review and editing.

Conflict of interest. The authors declare no conflict of interest.

Funding. This research did not receive any specific external funding.

Data availability. The data supporting the findings are available within the article; simulation files and calculation sheets are available from the corresponding author on reasonable request.

Use of AI tools. Generative AI tools were used to improve language and to check calculations and references. The authors reviewed all content and take full responsibility for the work.

REFERENCES

[1] IEA, The Future of Cooling: Opportunities for Energy-Efficient Air Conditioning, International Energy Agency, Paris, 2018. Available: https://www.iea.org/reports/the-future-of-cooling

[2] M. Lachheb, Z. Younsi, N. Youssef, S. Bouadila, Enhancing building energy efficiency and thermal performance with PCM-integrated brick walls: A comprehensive review, Building and Environment, 256, 2024, 111476. doi: 10.1016/j.buildenv.2024.111476

[3] A. Jurizat, Penurunan temperatur ruang dalam dengan menggunakan dinding massa termal internal di rumah bata, Master's thesis, Department of Architecture, Institut Teknologi Bandung, Bandung, 2019.

[4] H. M. Teamah, M. Teamah, Phase change materials integration in building envelopes under different climatic conditions: State of the art, opportunities, and challenges, Energy Storage, 7(5), 2025, e70250. doi: 10.1002/est2.70250

[5] A. Yadav, A. K. Pandey, M. Samykano, B. Kalidasan, Z. Said, A review of organic phase change materials and their adaptation for thermal energy storage, International Materials Reviews, 69(7–8), 2024, pp. 380–446. doi: 10.1177/09506608241292406

[6] J. Lei, J. Yang, E.-H. Yang, Energy performance of building envelopes integrated with phase change materials for cooling load reduction in tropical Singapore, Applied Energy, 162, 2016, pp. 207–217. doi: 10.1016/j.apenergy.2015.10.031

[7] C. Eller, M. Rida, K. Boudier, C. Otoni, G. Celani, L. Labaki, S. Hoffmann, Climate-based analysis for the potential use of coconut oil as phase change material in buildings, Sustainability, 13(19), 2021, 10731. doi: 10.3390/su131910731

[8] S. Kahwaji, M. A. White, Edible oils as practical phase change materials for thermal energy storage, Applied Sciences, 9(8), 2019, 1627. doi: 10.3390/app9081627

[9] S. Wonorahardjo, I. M. Sutjahja, D. Kurnia, Z. Fahmi, W. A. Putri, Potential of thermal energy storage using coconut oil for air temperature control, Buildings, 8(8), 2018, 95. doi: 10.3390/buildings8080095

[10] S. Wonorahardjo, I. M. Sutjahja, D. Kurnia, Potential of coconut oil for temperature regulation in tropical houses, ***Journal of Engineering Physics and Thermophysics***, 92(1), 2019, pp. 80–88. doi: 10.1007/s10891-019-01909-7

[11] W. A. Putri, Z. Fahmi, I. M. Sutjahja, D. Kurnia, S. Wonorahardjo, Thermophysical parameters of coconut oil and its potential application as the thermal energy storage system in Indonesia, ***Journal of Physics: Conference Series***, 739, 2016, 012065. doi: 10.1088/1742-6596/739/1/012065

[12] A. Li, Y. Yang, Y. Ren, Y. Wan, W. Wu, H. Zhang, Bio-based composite phase change material utilizing wood fiber and coconut oil for thermal management in building envelopes, ***Journal of Cleaner Production***, 469, 2024, 143177. doi: 10.1016/j.jclepro.2024.143177

[13] A. Ismail, J. Wang, B. A. Salami, L. O. Oyedele, G. K. Otukogbe, Microencapsulated phase change materials for enhanced thermal energy storage performance in construction materials: A critical review, Construction and Building Materials, 401, 2023, 132877. doi: 10.1016/j.conbuildmat.2023.132877

[14] H. Jiang, C. Yang, J. Song, P. J. Cao, J. Chen, J. Wang, W. Hong, Efficient enhancement of heat storage capacity of polyethylene glycol phase change material based on a novel fly ash support, ACS Sustainable Chemistry & Engineering, 12(19), 2024, pp. 7382–7391. doi: 10.1021/acssuschemeng.4c00354

[15] P.-E. Bat-Erdene, S. Pareek, Experimental study on the development of fly ash foam concrete containing phase change materials (PCMs), Materials, 15(23), 2022, 8428. doi: 10.3390/ma15238428

[16] A. de Gracia, Dynamic building envelope with PCM for cooling purposes – Proof of concept, Applied Energy, 235, 2019, pp. 1245–1253. doi: 10.1016/j.apenergy.2018.11.061

[17] S. Zhou, M. Song, K. Shan, L. Zhang, B. You, A. G. Razaqpur, Heating and energy performances of a dynamic Trombe wall incorporating phase change materials under different operation modes, ***Journal of Building Engineering***, 95, 2024, 110201. doi: 10.1016/j.jobe.2024.110201

[18] Government of the Republic of Indonesia, Peraturan Pemerintah Nomor 22 Tahun 2021 tentang Penyelenggaraan Perlindungan dan Pengelolaan Lingkungan Hidup, Lembaran Negara Republik Indonesia Tahun 2021 Nomor 32, Jakarta, 2021.

[19] A. Widayanti, R. A. A. Soemitro, H. Suprayitno, J. J. Ekaputri, Characterization and compressive strength of fly ash based-geopolymer paste, MATEC Web of Conferences, 195, 2018, 01023. doi: 10.1051/matecconf/201819501023

[20] L. Atmaja, H. Fansuri, A. Maharani, Crystalline phase reactivity in the synthesis of fly ash-based geopolymer, ***Indonesian Journal of Chemistry***, 11(1), 2011, pp. 90–95. doi: 10.22146/ijc.21426

[21] A. Jurizat, G. Kresnadian, F. M. Ikhsanudin, Peningkatan kemampuan minyak kelapa sebagai phase change material dengan menggunakan fly ash untuk mengendalikan temperatur ruang dalam, Bukit Asam Innovation Award 2022: Greenovator, Bandung, 2022.

[22] A. Jurizat, H. Andoni, I. M. Sutjahja, Cell sizes study of encapsulated coconut oil for heat exchanger application, in: Proceedings of the International Conference on Building Science and Technology, Bandung, 2018.

[23] J. Wang, J. K. Carson, M. F. North, D. J. Cleland, A new approach to modelling the effective thermal conductivity of heterogeneous materials, ***International Journal of Heat and Mass Transfer***, 49(17–18), 2006, pp. 3075–3083. doi: 10.1016/j.ijheatmasstransfer.2006.02.007

[24] D. P. Bentz, M. A. Peltz, A. Durán-Herrera, P. Valdez, C. A. Juárez, Thermal properties of high-volume fly ash mortars and concretes, ***Journal of Building Physics***, 34(3), 2011, pp. 263–275. doi: 10.1177/1744259110376613

[25] V. Alexiades, A. D. Solomon, Mathematical Modeling of Melting and Freezing Processes, Hemisphere Publishing Corporation, Washington, DC, 1993.

[26] Ladybug Tools, Butterfly: A plugin to create and run OpenFOAM cases from Grasshopper and Dynamo, source code (recipe.py, turbulenceProperties.py). Available: https://github.com/ladybug-tools/butterfly

[27] Badan Standardisasi Nasional, SNI 03-6572-2001: Tata cara perancangan sistem ventilasi dan pengkondisian udara pada bangunan gedung, BSN, Jakarta, 2001.

[28] ASHRAE, ANSI/ASHRAE Standard 55-2020: Thermal Environmental Conditions for Human Occupancy, American Society of Heating, Refrigerating and Air-Conditioning Engineers, Atlanta, 2020.

[29] Z. Abilkhassenova, S. A. Memon, A. Ahmad, A. Saurbayeva, J. R. Kim, Utilizing the Fanger thermal comfort model to evaluate the thermal, energy, economic, and environmental performance of PCM-integrated buildings in various climate zones worldwide, Energy and Buildings, 297, 2023, 113479. doi: 10.1016/j.enbuild.2023.113479

[30] Direktorat Jenderal Ketenagalistrikan, Faktor Emisi Gas Rumah Kaca Sistem Ketenagalistrikan Tahun 2019, Kementerian Energi dan Sumber Daya Mineral, Jakarta, 2019; established by Keputusan Menteri ESDM Nomor 163.K/HK.02/MEM.S/2021.

[31] I. Febijanto, Perhitungan faktor emisi di sistem jaringan ketenagalistrikan Jawa-Madura-Bali, ***Jurnal Teknologi Lingkungan***, 11(2), 2010, pp. 227–237.

[32] Kementerian Energi dan Sumber Daya Mineral, Peraturan Menteri ESDM Nomor 8 Tahun 2023 tentang Perubahan atas Peraturan Menteri ESDM Nomor 28 Tahun 2016 tentang Tarif Tenaga Listrik yang Disediakan oleh PT Perusahaan Listrik Negara (Persero), Jakarta, 2023; tariff level for 2026 confirmed in Siaran Pers No. 102.Pers/04/SJI/2025, 31 December 2025.

[33] Kementerian Pekerjaan Umum dan Perumahan Rakyat, Peraturan Menteri PUPR Nomor 1 Tahun 2022 tentang Pedoman Penyusunan Perkiraan Biaya Pekerjaan Konstruksi Bidang Pekerjaan Umum dan Perumahan Rakyat, Kementerian PUPR, Jakarta, 2022.

[34] K. Faraj, M. Khaled, J. Faraj, F. Hachem, C. Castelain, A summary review on experimental studies for PCM building applications: Towards advanced modular prototype, Energies, 15(4), 2022, 1459. doi: 10.3390/en15041459

[35] A. Demirbaş, Fuel properties and calculation of higher heating values of vegetable oils, Fuel, 77(9–10), 1998, pp. 1117–1120. doi: 10.1016/S0016-2361(97)00289-5